Soil & Tillage Research 210 (2021) 104938

Contents lists available at ScienceDirect

Soil & Tillage Research

journal homepage: www.elsevier.com/locate/still

The effect of machine traffic zones associated with field headlands on soil structure in a survey of 41 tilled fields in a temperate maritime climate

Mark Ward [a,b,*], Kevin McDonnell [a], Konrad Metzger [c,d], Patrick Dermot Forristal [b]

[a] School of Agriculture and Food Science, UCD, Belfield, Dublin 4, Ireland
[b] Teagasc CELUP, Crops Research, Oak Park, Carlow, Ireland
[c] Environment, Soils and Land Use Department, Teagasc, Johnstown Castle Research Centre, Wexford, Ireland
[d] International Network for Environment and Health (INEH), School of Geography and Archaeology National University of Ireland, Galway, Ireland

ARTICLE INFO

Keywords:
Headland
Visual soil assessment
Soil structure
Compaction
Machinery traffic
Grain yield

ABSTRACT

Machinery traffic imposes a negative effect on soil structure, leading to soil compaction. Studies to date have primarily focused on the influence of applied wheel loads on soil structure. Few studies have assessed the impact of commercial farm operations on soil structure and crop performance, particularly on field headlands in a temperate maritime climate such as Ireland. A survey was conducted on 41 conventionally managed field sites to investigate the effect of field position (field edge, turning, transition and in-field zones) in relation to machinery operations on soil structure. Soil texture classes ranged from sandy loam to clay loam. All sites used plough-based crop establishment. Soil structural condition was assessed visually using the visual evaluation of soil structure method (VESS) for the topsoil (0−250 mm), and Double Spade below plough depth (250−400 mm). Quantitative soil measurements such as shear strength, bulk density and porosity using soil cores post-harvest, and soil cone penetration resistance were taken at two time points in the crop growth cycle. For most measurements of soil structure, the in-field zone of least machinery traffic produced the best scores (*Sq* 2.81 & *DS* 2.48), and the turning zone returned the poorest scores in the 0−250 mm soil layer (*Sq* 3.31 & *DS* 2.91). The strongest quantitative scores for the in-field and turning zones, respectively, were for trowel penetration resistance in the upper (2.49 & 3.20) and lower (3.41 & 4.05) soil depth layers and for shear vane (38.17 & 53.59 kPa) for the same zones. The visual assessments and some of the quantitative measurements (0−250 mm soil layer) followed the zone order trend of: turning, field edge, transition and in-field, for increasing machinery traffic. The results show that the visual soil indicators used in this study are more sensitive than quantitative soil measurements such as soil bulk density (ρb) or porosity (TP and MP) at detecting soil structural differences between zones, particularly below plough depth (>250 mm soil depth).

1. Introduction

In tilled fields, the area of land next to the boundary is commonly known as the 'headland' (Sparkes et al., 1998a; Wilcox et al., 2000; Welch et al., 2016; Ward et al., 2020). It typically extends to the first tramline parallel to the crop edge and contains all non-working machinery manoeuvres (Boatman and Sotherton, 1988; Boatman, 1992). According to Sparkes et al. (1998a) and Sparkes et al. (1998b), headlands can be categorised as 'turning headlands' where machinery turns occur resulting in damage to soil structure, or 'non-turning headlands' representing the remaining field headlands. In a survey, of commercial headland turning practices in tilled fields, some headland machinery turns drove over the same area of land up to three times (Burke et al., 2018). Some machinery manoeuvres executed on headlands adversely affect soil structural condition (Ansorge and Godwin, 2007; VDI, 2014). Soil structure is a key aspect of soil quality (Mueller et al., 2013) and refers to the physical organisation of soil aggregates (Emmet-Booth et al., 2019a). Changes in machinery travel direction cause horizontal soil disturbance whereas actual machine weight causes vertical soil disturbance (Bochtis and Vougioukas, 2008).

There has been a trend to use large efficient machinery (Kumhála et al., 2013) to increase productivity. However, with larg equipment, comes heavy axle loads leading to a greater risk of soil deformation, caused by the compounding stresses of powered, slipping, and heavily

* Corresponding author at: School of Agriculture and Food Science, UCD, Belfield, Dublin 4, Ireland.
E-mail address: mark.ward@ucdconnect.ie (M. Ward).

https://doi.org/10.1016/j.still.2021.104938
Received 19 December 2019; Received in revised form 4 November 2020; Accepted 12 January 2021
Available online 15 March 2021

loaded wheels (Ehlers and Goss, 2016). According to Chamen et al. (2006) and Kumhála et al. (2013), the average weight and power of agricultural machinery has increased three fold since 1966 while wheel loads have risen by a factor of six over the same period. Van den Akker and Schjønning (2004), stated that high tractor wheel loads of 50 kN that caused initial soil structural damage in the form of subsoil compaction in the 1980's have since been replaced with 90–120 kN wheel loads from self-propelled slurry tankers in the Netherlands and self-propelled sugar beet harvesters in Sweden. The risk of soil structural damage is generally greatest at high soil moisture contents but this may also vary according to soil texture, tyre ground pressures and the number of machine passes over the same area of soil (Muckel and Mausbach, 1996). Botta et al. (2004) considered compaction caused by agricultural traffic to be primarily caused by excessive axle loads, high tyre ground pressures and the intensity or repeated trafficking of the soil for tramline work and harvest operations. This was also noted by Burke et al. (2018) where rear axle loads ranged from 5.88 to 16.05 t producing predicted soil stresses from 72 to 125 kPa and demonstrated the forces that some soils are subject to. As machine weights have increased, wide tyres with low inflation pressures have enabled mean ground contact pressures to remain approximately constant (Alakukku et al., 2003; VDI, 2014). Botta et al. (2009) also documented the effects of repeated wheelings with low wheel and axle loads on subsoils. However, subsoil stress is influenced more by axle load (Botta et al., 2013) or wheel load (Alakukku et al., 2003) than contact pressure.

Machinery traffic has given rise to soil structural decline in the form of both topsoil (typically 0−300 mm) and subsoil (typically >300 mm) compaction (Batey, 2009; Newell-Price et al., 2013). On agricultural field headlands, the ability of roots to grow, the percentage of large pores, the macropore size distribution and gas diffusion of the soil may be impacted (Allmaras et al., 1988). Compacted soils have a higher mass per unit volume and reduced pore volume than well-structured soils (Van den Akker and Schjønning, 2004; Batey, 2009). During the compaction process, soil aggregates and particles can become rearranged or smeared (Scholefield and Hall, 1985) and a reduction in the size and continuity of soil pores will affect a soil's ability to deliver key ecosystem services (Newell-Price et al., 2013). Reduced nutrient cycling and water infiltration on headlands also contribute to reduced productivity (Ishaq et al., 2001a, b). Subsoil compaction caused by heavy machinery with high axle loads has been reported (Arvidsson and Keller, 2007). As depth increases, there is a decrease in the rate at which self-amelioration of compacted soils occur (McHugh et al., 2009). The effects of subsoil compaction are long lasting (Håkansson and Medvedev, 1995; Alakukku et al., 2003).

Soil structural assessments can be used by growers to assess how their management practices are impacting soil quality (Vieweger, 2016) to allow for the early detection of developing compaction problems (Askari et al., 2013). Despite concerns of subjectivity (Mueller et al., 2009; Askari et al., 2013), Visual Soil Evaluation (VSE) methods can reliably provide a semi-quantitative in-field soil structural assessment (Askari et al., 2013; Ball et al., 2015; Emmet-Booth et al., 2018; Murphy et al., 2013). A rating score, based on visual indicators of macro-morphological soil characteristics is assigned (Emmet-Booth et al., 2016). VSE techniques can be categorised into spade or profile methods, each exploring a different depth in the soil profile (Emmet--Booth et al., 2016). VESS (Guimarães et al., 2011) is a widely accepted spade method, while Double Spade (DS) (Emmet-Booth et al., 2019a) is a more recent variant that bridges both spade and profile approaches when considering soil to 400 mm depth. They are easy to learn, use, and produce ordinally scaled scores allowing for comprehensive statistical analysis and an overall conclusion on soil structural quality (Mueller et al., 2009).

Many studies use bulk density, shear resistance and soil cone penetration resistance as primary indicators of physical soil structural condition (Logsdon and Cambardella, 2000; Mueller et al., 2009). However, these structural indicators can be impacted by soil moisture or texture (To and Kay, 2005; Mueller et al., 2009). Soil bulk density is frequently used to express soil structural quality and is estimated as soil mass per unit of occupied volume (Bachmann and Hartge, 2006; Bartholomew and Williams, 2010; Emmet-Booth et al., 2019a). It is generally impacted by factors such as soil texture, soil structure, soil organic matter or clay content (Bachmann and Hartge, 2006; Newell-Price et al., 2013). Increased bulk densities represent reduced soil porosity (Bartholomew and Williams, 2010) and infiltration capacity (Anken et al., 2016) associated with reduced plant growth due to restricted drainage or by directly impeding root penetration (Cook et al., 1996). Increased density is usually traffic related, either as machinery traffic (Anken et al., 2016) or through trampling by livestock (Bell et al., 2011). Emmet-Booth et al. (2019a) used bulk density to 400 mm soil depth to validate the DS methodology.

Headlands are considered to be "low productivity" field areas (Bochtis and Vougioukas, 2008). Reduced soil structural quality limits gas exchange capacity between the soil and the atmosphere, thus reducing water and nutrient absorption rates necessary for plant root growth (VDI, 2014). Research has demonstrated the negative impact of machinery traffic on crop performance (Arvidsson and Håkansson, 2014; Emmet-Booth et al., 2019b). Previous research typically compares headlands with in-field areas as a binary comparison (Boatman, 1992; Sparkes et al., 1998a; Emmet-Booth et al., 2019a), or as an area where soil structure, crop performance or other factors vary as a simple function of distance from the field edge (Speller et al., 1992; Cook and Ingle, 1997; Wilcox et al., 2000; Kuemmel, 2003). On a limited study of ten tilled field headlands in Ireland (Emmet-Booth et al., 2019a), contrasting visual soil scores between headlands, and in-field areas were documented in a binary fashion (mean VESS *Sq* 3.0 and 2.6; DS 2.8 and 2.2, for headland and in-field areas respectively). In studies that evaluated crop performance on headlands, a general trend for yields to increase with distance from the field boundary was noted (Speller et al., 1992; Cook and Ingle, 1997; Wilcox et al., 2000; Kuemmel, 2003). However, such methodologies fail to consider that different headland areas are subject to contrasting stresses, primarily due to machinery operations (Ward et al., 2020).

As traffic associated with plough based crop establishment systems on headlands is not evenly distributed, or its intensity does not decline in a simple relationship with distance from the field edge, an alternative zone approach was developed (Ward et al., 2020) and used to analyse crop performance. Individual zones based on traffic densities were assigned to specific headland areas and an in-field area for comparison. In that work, the lowest grain yields were recorded next to the field boundary, whereas the best yields were at the in-field areas. While previous studies investigated spatial variability in crop performance (Wilcox et al., 2000; Ward et al., 2020) or soil strength (To and Kay, 2005) in isolation on headlands, there are few studies which combined both.

The need to monitor and assess soil structural condition is important (Mueller et al., 2013). This is particularly true where the headland impact is substantial. Here, wetter soils, smaller fields and the use of tractor-mounted rather than trailed implements, can result in a greater risk of soil structural damage on field headlands. Furthermore, there is a dearth of studies in a temperate maritime climate, such as Ireland, that systematically study headland soil structural condition. Even though studies document the impact of headlands on crop performance (Wilcox et al., 2000; Kuemmel, 2003; Ward et al., 2020) and to a limited extent, soil structure (Wilcox et al., 2000; Emmet-Booth et al., 2019a), and the negative yield effect of traffic induced soil compaction (Håkansson, 2005; Arvidsson and Keller, 2007; Arvidsson and Håkansson, 2014), little evidence exists to link crop and soil effects recorded on field headlands with areas of specific machinery operations. Without this evidence, it is challenging to ascribe crop effects on headlands to a specific causative factor.

There are knowledge gaps in the areas of soil structural conditions in zones associated with machine traffic patterns on field headlands, soil

structural condition in the headland areas of tillage fields in a temperate maritime climate, and, the association between soil structural condition and crop yields. The objective of this study was to analyse and quantify the impact of machinery traffic on soil structural condition in terms of visual and quantitative soil assessments at specific field positions on tillage fields in a temperate maritime climate, and to determine the impact of soil structural condition on crop performance. The primary hypotheses to be tested were that soil structural condition on field headlands differs between zones designated by machinery operations, and, that the zone of poorest soil structure produces the lowest crop yield.

2. Materials and methods

2.1. Site selection

Forty one fields from twenty five farms in a temperate maritime climate in Ireland were selected for the survey. They were sourced through regional Teagasc tillage advisors. Teagasc is a semi-state authority in Ireland that conducts research, and provides advice and training services in the agri-food sector and has 2379 cereal grower clients (Teagasc, 2018). Sites were located from an area east of 53°54′N 6°25′W in the North-East of Ireland to 52°06′N 7°48′W in the South which is the primary cereal growing region of Ireland (Kennedy, 2015). All fields were managed under conventional cultivation (mouldboard plough based primary cultivation to 200−250 mm depth) and subject to continuous annual cropping of cereals for at least the previous three years and included a soil texture typical of tilled soils in Ireland. The mean field size was 8.57 ha (range: 1.64–37.72 ha), and the mean elevation was 64.4 m (range: 17–125 m). Soil texture was characterized according to USDA (2018), and included clay loam, loam and sandy loam soil textural types (Tables 1–3). In the current paper, soil textures 1 and 2 refer to the soil textures found at 0−250 and 250−400 mm sample depths respectively.

2.2. Experimental design

The experimental fieldwork was conducted in the autumns of 2016 and 2017. The post-harvest period was chosen as it was most likely to have relatively stable soil moisture conditions, unlike late autumn or spring periods where changes in soil moisture during the site survey process would make soil assessment comparisons between sites difficult. In year one, 21 field headlands where machine turning occurred were surveyed, followed by 20 in year two. Following an assessment of headland turning techniques at each site with growers, the novel zone approach as described by Ward et al. (2020) based on machine traffic intensities was applied. Zones influenced by implement size, bout widths and turning techniques were set out parallel to the field edge at one of the machine-turning headlands (Fig. 1). The ‘field edge’ was the closest to the boundary and had moderate headland traffic, the ‘turning’ zone had most headland traffic and highest axle loads, the ‘transition’ zone was between the turning and in-field area, and, the ‘in-field’ zone was the internal field area and was used as a control to which the other zones were compared. The dimensions of the zones varied with field tramline bout width, machine widths and associated turning practice (Table 4). In a 24 m tramline system for example which was the most commonly encountered system, where all tractor mounted equipment is raised and axle loads are greatest at a position approximately 12 m from the field boundary, sample points within the zones were positioned at 3 m from the boundary (representing a mid-point in the field edge zone), at 8.5 m (turning area), at 16 m (transition zone) and at 35 m (in-field zone) from the field boundary along each transect. With four sampling transects across the zones (replications) this resulted in 16 sample areas per site” (Fig. 1). The distance between transects was determined by tramline bout widths, typically 24 m (range: 15–30 m), used by individual growers. This research approach has the potential to identify the factors within each zone that may impact on soil structure, and offer opportunities to address management within those zones.

Table 1
Table of Winter Barley (n = 8) site locations and soil texture 1 (0-250 mm soil depth).

Longitude, Latitude	Sand (%)	Silt (%)	Clay (%)	Soil Texture 1 (USDA)
52°48′ N, 6°51′ W	65	21	14	Sandy loam
52°58′ N, 6°59′ W	53	31	16	Sandy loam
53°18′ N, 6°39′ W	36	40	24	Loam
53°19′ N, 6°39′ W	41	37	22	Loam
53°51′ N, 6°27′ W	43	33	24	Loam
52°49′ N, 6°48′ W	56	30	14	Sandy loam
52°55′ N, 6°56′ W	56	27	17	Sandy loam
53°54′ N, 6°25′ W	44	36	20	Loam

Table 2
Table of Spring Barley (n = 8) site locations and soil texture 1 (0-250 mm soil depth).

Longitude, Latitude	Sand (%)	Silt (%)	Clay (%)	Soil Texture 1 (USDA)
52°43′ N, 6°50′ W	65	21	14	Sandy loam
53°49′ N, 6°25′ W	44	34	22	Loam
52°08′ N, 7°48′ W	49	32	19	Loam
52°58′ N, 6°59′ W	56	30	14	Sandy loam
52°43′ N, 6°50′ W	65	22	13	Sandy loam
52°32′ N, 6°37′ W	32	41	27	Clay loam
52°31′ N, 6°36′ W	29	38	33	Clay loam
52°52′ N, 6°58′ W	40	37	23	Loam
52°52′ N, 6°58′ W	42	36	22	Loam
52°52′ N, 6°54′ W	57	25	18	Sandy loam
52°32′ N, 6°37′ W	33	37	30	Clay loam
52°31′ N, 6°36′ W	31	38	31	Clay loam
52°24′ N, 6°26′ W	74	15	11	Sandy loam
52°31′ N, 6°29′ W	61	24	15	Sandy loam
52°55′ N, 6°05′ W	30	41	29	Clay loam
52°53′ N, 6°55′ W	47	32	21	Loam
52°55′ N, 6°56′ W	66	14	20	Sandy loam
53°00′ N, 7°04′ W	62	23	15	Sandy loam
52°59′ N, 6°59′ W	59	25	16	Sandy loam
52°47′ N, 6°54′ W	62	23	15	Sandy loam
52°31′ N, 6°29′ W	60	25	15	Sandy loam
52°45′ N, 6°48′ W	60	28	12	Sandy loam
52°42′ N, 6°55′ W	52	31	17	Loam
52°32′ N, 6°36′ W	31	41	28	Clay loam

Table 3
Table of Winter Wheat (n = 24) site locations and soil texture 1 (0-250 mm soil depth).

Longitude, Latitude	Sand (%)	Silt (%)	Clay (%)	Soil Texture 1 (USDA)
52°51′ N, 6°52′ W	65	23	12	Sandy loam
53°30′ N, 6°14′ W	35	41	24	Loam
52°08′ N, 7°49′ W	52	31	18	Loam
52°06′ N, 7°48′ W	52	32	16	Loam
53°39′ N, 6°36′ W	38	37	25	Loam
53°44′ N, 6°30′ W	33	41	26	Loam
53°32′ N, 6°19′ W	43	35	22	Loam
53°32′ N, 6°19′ W	42	38	20	Loam

2.3. Visual soil assessment

In the current study, VESS (Ball et al., 2007; Guimarães et al., 2011) and Double Spade (DS) (Emmet-Booth et al., 2019a) were the visual soil evaluation methods chosen as they are influenced by a range of soil properties (aggregate size and shape, soil porosity, strength, roots and biological activity) and integrate the assessment of various soil structure characteristics into a single score value. All visual assessments were carried out by the same assessor. VESS was conducted at the 0−250 mm

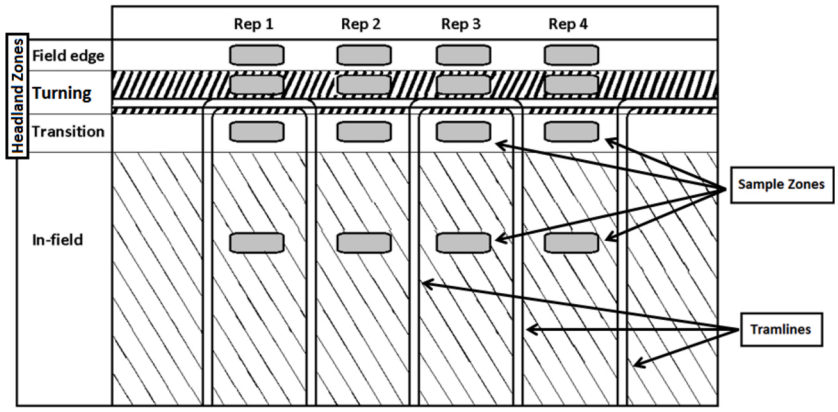

Fig. 1. Illustration of zone approach and sample locations in grey (Ward et al., 2020).

Table 4
Dimensions of the four headland zones as determined by bout width, machinery size and type and associated turning practice.

Tramline bout widths (m)	Primary cultivations	Primary cultivations	Seed drill		Headland Zone Dimensions Distance from field boundary (m)			
	Plough (furrow #)	Cultivator width (m)	Variant	Width (m)	Field Edge	Turning	Transition	In-field
18	3	3	Mounted	3	0–4	4–11	11–14	24–29
24	5	3	Mounted	3	0–5	5–14	14–17	35–38
24	5	4	Mounted	4	0–5	5–14	14–17	35–38
24	5	6	Trailed	3	0–4	4–14	14–17	35–38
27	5	3	Mounted	3	0–5	5–15	15–18	37–40
30	7	6	Trailed	6	0–6	6–17	17–20	39–42

soil depth in the cultivated layer. At a sample point in the field edge, turning, transition and in-field zones for each replicate, intact sample blocks to a soil depth of ~250 mm were extracted using a spade and were broken up by hand to reveal the presence of any structural layers and to assess soil structural characteristics according to the VESS score-sheet (Guimarães et al., 2011), assessing for soil porosity, aggregate characteristics and root growth. In the 0−250 mm soil layer, for greater data collection accuracy, a modified VESS *Sq* scoring protocol was used. On a scale of 1–5, with lower scores indicating better soil structural quality, a resolution of 0.25 score units (e.g. 3.0, 3.25, 3.5, 3.75, 4 etc.) was used to score soil blocks.

In the deep uncultivated soil layer, at 250–400 mm from the soil surface, a slightly modified version of the DS (Emmet-Booth et al., 2019a) visual evaluation method was conducted at each sample point to evaluate soil structure. Soil pits of ≈450 mm were excavated to allow ease of access to the 400 mm profile face. The modification to the method involved an assessment of the percentage of the aggregates which were in the size categories 0−30 mm, 30−50 mm and 50−80 mm to provide a better quantifiable mean 'aggregate/ fragment size' value. A component of the DS (Emmet-Booth et al., 2019a) visual method, trowel penetration resistance (TPR) was also recorded separately to give additional parameters within the 0−250 mm (TPR 1) and 250−400 mm (TPR 2) soil layers.

2.4. Quantitative soil measurements

2.4.1. Field sampling

At each of the 16 sample points, located in the field edge, turning, transition and in-field zones across every field headland, intact soil bulk density core ring samples (Ø 50 mm x h 50 mm) were inserted vertically at depths centred at 125 mm and 325 mm, for subsequent porosity measurements. The samples were foil wrapped and sealed in a polythene bag. A (Ø 70 mm x h 70 mm) non-intact sample for bulk density analysis was also taken centred at 325 mm depth. All soil samples were stored at 4 °C until laboratory processing.

Soil strengths were measured within a 2 m radius of each of the sixteen sample points. Cone penetration resistance (CPR) was measured at 10 points with an Eijkelkamp recording cone penetrometer at incremental depths of 10 mm–600 mm using a 100 mm^2, 60° angle cone, as used in numerous studies (Tebrügge and Düring, 1999; Hanse et al., 2011; O'flynn et al., 2014; Emmet-Booth et al., 2019a). CPR measurements were taken post-harvest in September (CPR A) and again in February (CPR B) when soil moisture was close to field capacity. Mean soil strength measurements for CPR at 0−250, 250−400 and 400−600 mm were calculated. Post-harvest, soil shear resistance (SR) was measured vertically with a 19 mm shear vane inserted to a depth of 150 mm.

2.4.2. Laboratory analysis

The intact soil core samples in the sample rings were stored at < 4 °C prior to analysis. Following the procedure of Emmet-Booth et al. (2019a), a 53 µm sieve mesh was attached to the bases using stainless steel jubilee clips. Samples were placed on a mesh rack in a sealable water tank in the cool room at 4 °C, and the water level brought up to within ≤ 1 mm of the sample surfaces for 64 h to ensure they were saturated. After saturation, the water level was lowered (but not emptied to maintain atmospheric conditions) and core samples allowed drain for 24 h. Samples were then placed in a forced draft oven at 105 °C for 48 h. Sample masses at each stage were determined to allow bulk density (ρb) according to Grossman and Reinsch (2002), and saturated volumetric water content (θSat) and consequently total porosity (TP), according to Emmet-Booth et al. (2019a) be determined. The proxy (θSat – θ24 h Drainage) which Emmet-Booth et al. (2019a) used to estimate macroporosity (MP), where all macropores (soil pores with an equivalent diameter >60 µm, from which water drains readily by gravity (Brady et al., 2008)) were considered to have drained following 24 h gravitational drainage was used. Finally, samples were re-soaked and sieved down to 2 mm to remove stones to allow ρb to be determined. Non-intact core samples where the sampled soil volume was pressed from the sampling cylinder into a bag, were dried, adjusted for

stone content and analysed for ρb. Henceforth ρb will refer to $\rho b_{2\ mm}$.

2.5. Soil structural condition and crop performance

To determine the impact of soil structural quality on crop yields, yield data for 40 of the 41 sites from Ward et al. (2020) was considered. In that study, yields of winter and spring barley, and winter wheat were determined using a detailed hand-harvesting method. At each zone, five randomly placed quadrat (0.125 m^2) samples were cut at ground level. They were subsequently threshed and cleaned. Yields (t/ha) were expressed at 85 % dry matter.

2.6. Statistical analyses

As each site had replicated measurements, both individual site and group analyses were possible. While visual scores for VESS and *DS* were assigned using a detailed scorecard, prior to conducting an analysis of variance (ANOVA), the assumptions of the analysis were first verified where residual checks were made (normal distribution, constant variance, etc.). This data was normally distributed and allowed analysis for parametric data to be applied.

The PROC GLIMMIX procedure in SAS 9.4 was used for a 2-way ANOVA structure with blocking to analyse the responses. Both years of the study were analysed together, but as different sites were monitored each year, it was not possible to analyse year as a factor. The factors employed were headland traffic zone, site (and its proxies of soil texture) with blocks nested within site. The means were compared using a Tukey adjustment for multiplicity effects.

To examine the impact of soil structure on crop performance, a multiple linear regression predictor model was also constructed in SAS 9.4 using the PROC GLMSELECT procedure. It examined the combined impact of several soil factors together on crop yield. All visual and quantitative scores were included in the selection set for the models. Crop yields were modelled separately with best-fit models, and these were reduced to determine a best overall model.

3. Results

The visual and quantitative soil measurements analysed for all sites together for both years of this study are presented in Table 5. There were significant interactions for headland zone by soil texture for a number of the measured parameters. The main effects of headland zone and soil texture were highly significant for most parameters measured. In the following sections, the interactions are considered with the appropriate main effect.

3.1. Visual soil assessments

Mean VESS *Sq* and *DS* assessment values per field zone are outlined in Table 5. In Table 6 the number of sites which had statistically significant differences in selected soil measurements between the headland and in-field areas, is presented.

3.1.1. Visual evaluation of soil structure (VESS) method

Mean VESS *Sq* scores were impacted by the traffic zone from which they were taken (Table 5). The in-field zone had the lowest (better) mean *Sq* score (*Sq* 2.81), 15 % lower than the turning zone (*Sq* 3.31) that is subject to the greatest intensity of machinery traffic and highest axle loads. There was a trend for *Sq* scores to increase, implying poorer soil structural quality in the zone order of in-field, transition, field edge and turning, which coincided with increasing machine traffic intensities. Mean *Sq* scores differed significantly between the main headland zones at the field edge and turning zones, and the remaining transition and in-field zones. When individual sites were examined (Table 6), statistical difference between the in-field and field edge zones was documented at four sites, and for eleven sites between the turning and in-field zones.

Soil texture at 250−400 mm soil depth had a significant impact on VESS ($P < 0.01$) with sites on clay loam soils having statistically higher (inferior) *Sq* scores than the sites on loam or sandy loam soils.

3.1.2. Double spade (DS) method

In the 250−400 mm soil layer, zone had a significant impact on double spade (*DS*) scores (Table 5). The lowest (best) mean *DS* score was found at the in-field zone (*DS* 2.48) and the highest (worst) (*DS* 2.91) at the turning zone. In-field scores were 15 % lower (indicating better soil structural quality) than the turning zone for *DS*. The field edge and the turning zones differed significantly to the transition and in-field zones with increasing scores following the zone order trend of in-field, transition, field edge and turning zones.

Soil texture (soil textures 1 & 2) had an effect ($P < 0.001$) on *DS* with a zone and soil texture 1 interaction ($P < 0.01$) observed. On the clay loam sites, the field edge zone had higher *DS* scores indicating poorer soil structure, than the other zones, whereas on the loam and sandy loam sites the turning area tended to have the highest scores (poorest structure) (Table 7). With the exception of the turning zone, the highest values for all other zones (field edge, transition and in-field) were recorded for clay loam sites.

The TPR component of *DS*, at both soil depths (0−250 and 250−400 mm) was impacted by zone ($P < 0.001$). The turning zone had the highest (poorest) TPR readings. At the 0−250 mm soil depth (TPR 1), the in-field zone gave the lowest (best) readings, while the transition zone gave the lowest values at 250−400 mm soil depth (TPR 2). Soil texture (soil textures 1 & 2) impacted on all TPR measurements. An interaction between soil texture 1 (0−250 mm from the soil surface) and TPR 2 was also noted (Table 8). The sandy loam sites tended to display the best TPR 2 values for all headland zones when compared against the other soil textures. Highest mean TPR 2 zone values for the field edge and turning areas were recorded for clay loam, and the transition and in-field zones for loam.

3.2. Quantitative soil measurements

Traffic zones influenced soil bulk densities (ρb) in the 0−250 mm soil layer, where the highest value (1.33 g/cm^3) was recorded at the turning zone and the lowest (1.27 g/cm^3) at the in-field zone. This in-field area also had lower bulk densities than the field edge, with a trend of increasing densities observed in the zone order of: in-field, transition, field edge and turning. In the 250−400 mm soil layer, statistical difference was not found between zones for the Ø 50 mm (ρb50) or Ø 70 mm (ρb70) bulk density analysis.

Headland traffic zones had an impact on total porosity (TP) at both 0−250 mm (TP 1) ($P < 0.001$) and 250−400 mm (TP 2) ($P < 0.01$) soil depth. The in-field zone produced the best TP 1 values but the poorest TP 2. For soil texture 1, statistical difference was documented between all three soil types with the clay loam soils producing the best mean TP and the sandy loams the poorest. In the case of soil texture 2, the sandy loam soils produced statistically lower TP than the clay loam or loam soils.

There was a zone and soil texture 1 interaction noted for macro porosity (MP) at 0−250 mm soil depth (MP 1). With the exception of the turning zone where the lowest MP was recorded (Table 9), clay loam had the highest MP for the field edge, transition and in-field zones. The sandy loam had the highest turning zone MP.

3.3. Soil strength measurements

Significant differences ($P < 0.001$) in mean shear resistance (SR) was observed between all zones at 150 mm soil depth. The in-field zone produced the best (lowest) SR values (38.17 kPa) while the turning zone gave the poorest (highest) readings (53.59 kPa), 40 % greater, indicating a higher soil strength. A zone and soil texture 1 interaction ($P < 0.001$) was observed (Table 10) indicating that for all soil textures, the highest SR measurements were recorded at the turning zone, while

Table 5
The effect of zone, soil texture 1 and soil texture 2 on visual and quantitative indicators of soil structural condition from survey sites (values followed by the same letter in each column are not significantly different).

		VESS (*Sq*) *DS*	TPR 1	TPR 2	SR (kPa)	ρb50 (0−250 mm) (g/cm^3)	ρb50 (250−400 mm) (g/cm^3)	ρb70 (250−400 mm) (g/cm^3)	TP 1 (0−250 mm) (%)	TP 2 (250−400 mm) (%)	MP 1 (0−250 mm) (%)	MP 2 (250−400 mm) (%)	CPR A (0−250 mm) (MPa)	CPR A (250−400 mm) (MPa)	CPR A (400−600 mm) (MPa)	CPR B (0−250 mm) (MPa)	CPR B (250−400 mm) (MPa)	CPR B (400−600 mm) (MPa)
Zone	**Field Edge**	3.18^{a}	2.95^{b}	3.89^{a}	50.72^{b}	1.31^{ba}	1.38^{a}	1.39^{a}	47.82^{bc}	44.44^{a}	1.58^{a}	1.46^{a}	1.99^{a}	3.56^{a}	2.54^{a}	1.78^{a}	3.77^{a}	3.92^{a}
	Turning	3.31^{a}	3.20^{a}	4.05^{a}	53.59^{a}	1.33^{a}	1.40^{a}	1.40^{a}	47.21^{c}	43.67^{ba}	1.51^{a}	1.52^{a}	2.04^{a}	3.52^{a}	2.45^{a}	1.83^{a}	3.76^{a}	4.10^{a}
	Transition	2.94^{b}	2.62^{c}	3.39^{b}	43.76^{c}	1.29^{bc}	1.40^{a}	1.42^{a}	48.36^{ba}	43.06^{b}	1.45^{a}	1.50^{a}	1.83^{b}	3.47^{ba}	2.49^{a}	1.82^{a}	3.66^{a}	3.99^{a}
	In-field	2.81^{b}	2.49^{c}	3.41^{b}	38.17^{d}	1.27^{c}	1.41^{a}	1.41^{a}	48.71^{a}	42.76^{b}	1.45^{a}	1.42^{a}	1.73^{c}	3.35^{b}	2.49^{a}	1.70^{b}	3.64^{a}	3.87^{a}
Texture 1 (0−250 mm soil depth)	**Clay loam (n = 6)**	3.13^{a}	2.97^{a}	3.83^{a}	52.00^{a}	1.11^{c}	1.22^{b}	1.24^{b}	52.60^{a}	47.25^{a}	1.96^{a}	1.42^{b}	2.12^{a}	3.62^{a}	2.45^{a}	2.21^{a}	4.28^{a}	4.04^{a}
	Loam (n = 18)	3.05^{a}	2.89^{a}	3.75^{a}	43.93^{c}	1.31^{b}	1.42^{a}	1.42^{a}	47.98^{b}	43.81^{b}	1.38^{b}	1.35^{b}	1.80^{c}	3.47b	2.50^{a}	1.64^{c}	3.59^{b}	4.02^{a}
	Sandy loam (n = 17)	3.04^{a}	2.68^{b}	3.55^{b}	47.42^{b}	1.35^{a}	1.44^{a}	1.45^{a}	46.45^{c}	41.81^{c}	1.46^{b}	1.63^{a}	1.92^{b}	3.44b	2.45^{a}	1.78^{b}	3.63^{b}	3.88^{a}
Texture 2 (250−400 mm soil depth)	**Clay loam (n = 5)**	3.21^{a}	3.18^{a}	4.13^{a}	48.51^{a}	1.28^{b}	1.39^{ba}	1.40^{ba}	49.10^{a}	44.00^{a}	1.64^{a}	1.25^{b}	1.97^{a}	3.47^{a}	2.14^{b}	1.89^{a}	3.92^{a}	4.04^{a}
	Loam (n = 19)	2.99^{b}	2.83^{b}	3.71^{b}	44.38^{b}	1.27^{b}	1.38^{b}	1.38^{b}	48.68^{a}	44.88^{a}	1.52^{a}	1.32^{b}	1.83^{b}	3.48^{a}	2.46^{a}	1.84^{a}	3.71^{b}	3.92^{a}
	Sandy loam (n = 17)	3.09^{ba}	2.69^{c}	3.53^{c}	48.43^{a}	1.33^{a}	1.42^{a}	1.43^{a}	46.98^{b}	41.79^{b}	1.44^{a}	1.72^{a}	1.95^{a}	3.48^{a}	2.59^{a}	1.69^{b}	3.64^{b}	3.99^{a}
		Pr > F	Pr > F	Pr > F	Pr > F	Pr > F	Pr > F	Pr > F	Pr > F	Pr > F	Pr > F	Pr > F	Pr > F	Pr > F	Pr > F	Pr > F	Pr > F	Pr > F
Zone		<0.001	<0.001	<0.001	<0.001	<0.001	<0.001	0.077	0.345	<0.001	0.004	0.398	0.596	<0.001	<0.001	0.664	<0.001	0.088	0.076
Site		<0.001	<0.001	<0.001	<0.001	<0.001	<0.001	<0.001	<0.001	<0.001	<0.001	<0.001	<0.001	<0.001	<0.001	<0.001	<0.001	<0.001	<0.001
Zone*Site		<0.001	<0.001	<0.001	<0.001	<0.001	0.006	<0.001	0.011	<0.001	0.385	<0.001	0.055	<0.001	<0.001	0.034	<0.001	0.007	0.008
Soil Texture 1		0.415	<0.001	<0.001	<0.001	<0.001	<0.001	<0.001	<0.001	<0.001	<0.001	<0.001	<0.001	<0.001	0.005	0.667	<0.001	<0.001	0.103
Zone*Soil Texture 1		0.123	0.008	0.061	<0.001	<0.001	0.384	0.802	0.182	0.053	0.075	<0.001	0.708	0.398	0.107	0.668	0.805	0.617	0.106
Soil Texture 2		0.007	<0.001	<0.001	<0.001	<0.001	<0.001	<0.001	<0.001	<0.001	<0.001	0.137	<0.001	<0.001	0.986	<0.001	<0.001	<0.001	0.412
Zone* Soil Texture2		0.071	0.124	0.239	0.216	0.625	0.672	0.169	0.666	0.119	0.146	0.007	0.977	0.085	0.405	0.893	0.330	0.911	0.062

DS Double Spade visual soil assessment method.
TPR Trowel Penetration Resistance (1 and 2 refer to 0−250 & 250−400 mm sample depths).
SR Shear Resistance.
Pb Bulk Density.
TP Total Porosity (1 and 2 refer to 0−250 & 250−400 mm sample depths).
MP Macro Porosity (1 and 2 refer to 0−250 & 250−400 mm sample depths).
CPR Cone Penetration Resistance ("A" and "B" refer to timings 1 and 2, i.e. post-harvest in September and February).
Soil Texture (1 and 2 refer to 0−250 & 250−400 mm sample depths).

Table 6
The number of sites showing statistical difference between the Field Edge or the Turning zones and the In-field zones for selected soil measurements.

	Field Edge vs. In-field	Turning vs. In-field
VESS (*Sq*)	4	11
DS	12	15
SR	20	23

Table 7
DS zone scores for the 0-250 mm soil layer (soil texture 1) (values followed by the same letter in each column are not significantly different).

	Clay Loam (n = 6)	Loam (n = 18)	Sandy Loam (n = 17)
Field Edge	3.11[a]	2.78[b]	2.77[a]
Turning	2.93[ba]	2.97[a]	2.84[a]
Transition	2.67[bc]	2.53[c]	2.51[b]
In-field	2.61[c]	2.40[c]	2.52[b]

Table 8
TPR 2 zone values for the 0-250 mm soil layer (soil texture 1) (values followed by the same letter in each column are not significantly different).

	Clay Loam (n = 6)	Loam (n = 18)	Sandy Loam (n = 17)
Field Edge	4.42[a]	3.88[a]	3.65[a]
Turning	4.25[a]	4.09[a]	3.92[a]
Transition	3.33[b]	3.48[b]	3.31[b]
In-field	3.33[b]	3.54[b]	3.31[b]

Table 9
MP 1 (%) zone scores for the 0-250 mm soil layer (soil texture 1) (values followed by the same letter in each column are not significantly different).

	Clay Loam (n = 6)	Loam (n = 18)	Sandy Loam (n = 17)
Field Edge	5.28[a]	2.82[a]	3.28[a]
Turning	2.70[b]	3.14[a]	4.06[a]
Transition	3.83[ba]	2.73[a]	3.32[a]
In-field	3.46[ba]	2.91[a]	3.19[a]

Table 10
SR (kPa) measurements for the 0-250 mm soil layer (soil texture 1) (values followed by the same letter in each column are not significantly different).

	Clay Loam (n = 6)	Loam (n = 18)	Sandy Loam (n = 17)
Field Edge	59.52[a]	46.86[a]	51.71[a]
Turning	62.39[a]	49.20[a]	55.14[a]
Transition	45.29[b]	41.84[b]	45.24[b]
In-field	40.80[b]	37.84[c]	37.59[c]

the lowest were at the in-field zones. For all turning zones, the highest measured values were documented for clay loam. In both the loam and sandy loam soils there was a significant difference in SR readings between the in-field and transition areas. However, there was no difference between those zones for the clay loam sites.

The zones as determined by machine traffic patterns had an effect ($P < 0.001$) on cone penetration resistance (CPR) values to 400 mm soil depth in September (CPR A), and to 250 mm in February (CPR B). In the 0−250 mm soil layer, the greatest resistances were recorded at the turning zone (2.04 and 1.83 MPa for CPR A and CPR B respectively), whereas at 250−400 mm soil depth they were recorded at the field edge (3.56 and 3.77 MPa for CPR A and CPR B respectively). At the same depths, the in-field zones gave statistically the lowest CPR measurements for both sample timings. There was a general trend of increasing resistances from the in-field to field edge zones noted at both timings to 400 mm.

3.4. Grain yield models

The in-field and transition headland zones tended to give better indicators of soil quality and better crop performance than the field edge and turning zones for all three crop types (winter and spring barley, and winter wheat) (Table 11). Two grain yield regression models were developed and reduced using a multiple linear regression predictor model using soil structural quality measurements. The factors included were those which contributed most to the model.

In the first model, a visual assessment component was excluded while it was allowed in the second model. The first model included ρb 0−250 mm, CPR A 0−250 mm, CPR A 250−400 mm, CPR B 0−250 mm and CPR B 250−400 mm. Higher yield correlations were obtained for winter barley ($P < 0.001$; $r^2 = 34.2$ %) and winter wheat ($P < 0.001$; $r^2 = 40.6$ %) versus spring barley ($P < 0.001$; $r^2 = 19.4$ %). The second model considered *DS*, SR, CPR A 250−400 mm, CPR A 400−600 mm and CPR B 0−250 mm. It gave better grain yield correlations for winter wheat ($P < 0.001$; $r^2 = 44.1$ %) and spring barley ($P < 0.001$; $r^2 = 32.5$ %) compared to the first model, while a lower correlation for winter barley ($P < 0.001$; $r^2 = 23.7$ %) was recorded. While these correlations are not particularly strong, the impact of zones on soil structure and crop yield for all different crop types (Table 11), indicates poorer soil structure parameters and lower crop yield where traffic is greater when comparing the turning zone with the in-field zone. However, the lowest yield was recorded at the field edge zone which did not have the poorest soil structure values.

4. Discussion

The impact of spatial position or zone, associated with machinery working patterns within headlands, on soil structure in this study of 41 conventionally managed sites was clearly indicated.

Mean visual (VESS and Double Spade) and quantitative soil scores: trowel penetration resistance (TPR); bulk density (ρb 0−250 mm), and; shear resistance (SR), followed the same headland zone order of increasing scores (i.e. in-field, transition, field edge and turning). This supports the hypothesis that soil structure differs between zones designated by machinery operations. The zone of maximum headland traffic gave the poorest visual soil scores and demonstrated the effect of machinery traffic on soil structure as assessed by visual soil evaluation methods. As indicated by VESS and *DS*, soil structural values at the turning area were 15 % higher (poorer) than the in-field area. According to Ball et al. (2007), the recorded *Sq* values could be categorised as moderate to poor. Unlike the turning zone, no machinery manoeuvres occur at the in-field zone and it is therefore subject to the lowest axle loads, ground pressures and traffic intensities. In a method validation study by Emmet-Booth et al. (2019a), where turning and in-field areas were contrasted, better visual in-field scores (in-field *Sq* 2.6 vs. headland *Sq* 3.0) were also reported.

Cone penetration resistance (CPR) measurements adhered to the same zone trend of least machinery traffic (in-field) producing the best (lowest) resistance values. The main headland zones (the field edge and turning zones) gave the poorest (highest) values. The reduction in CPR strength values from September (CPR A) to February (CPR B) was noted for the 0−250 mm soil layer, while it tended to increase for the 250−400 mm soil layer. The results were probably due to the loosening that occurred during ploughing, as also observed by Schäfer-Landefeld et al. (2004) and possibly coupled with greater soil moisture in the upper layer. At the greater soil depth (250−400 mm soil layer), the impact of traffic still remained resulting in very high values, which, according to Berryman et al. (1982) may indicate dense soil. However, the potential impact of contrasting soil moisture contents between measurements must also be considered (VDI, 2014).

Table 11
The effect of zone on grain yields and soil structural quality measurements for each individual crop (values followed by the same letter in each column are not significantly different).

		Yield (t/ha)	VESS (*Sq*)	*DS*	SR (kPa)	pb50 (0−250 mm) (g/cm^3)	CPR A (0−250 mm) (MPa)	CPR A (250−400 mm) (MPa)	CPR A (400−600 mm) (MPa)	CPR B (0−250 mm) (MPa)	CPR B (250−400 mm) (MPa)	CPR B (400−600 mm) (MPa)
WB	Field Edge	10.98^{b}	2.75^{ba}	2.45^{b}	49.40^{a}	1.36^{a}	1.74^{a}	3.50^{a}	2.30^{a}	1.88^{a}	3.74^{a}	3.74^{a}
	Turning	11.45^{b}	2.98^{a}	2.70^{a}	53.33^{a}	1.36^{a}	1.75^{a}	3.37^{a}	2.15^{a}	1.83^{a}	3.62^{a}	4.12^{a}
	Transition	11.33^{b}	2.56^{b}	2.44^{b}	41.82^{b}	1.32^{a}	1.59^{b}	3.37^{a}	2.22^{a}	1.93^{a}	3.65^{a}	3.75^{a}
	In-Field	12.28^{a}	2.51^{b}	2.34^{b}	37.47^{c}	1.34^{a}	1.53^{b}	3.25^{a}	2.46^{a}	1.84^{a}	3.56^{a}	3.99^{a}
SB	Field Edge	6.45^{d}	3.21^{a}	2.91^{a}	53.57^{b}	1.28^{ba}	2.16^{a}	3.62^{a}	2.50^{a}	1.81^{a}	3.87^{a}	3.86^{a}
	Turning	7.19^{c}	3.35^{a}	2.93^{a}	56.51^{a}	1.31^{a}	2.22^{a}	3.58^{a}	2.42^{a}	1.88^{a}	3.92^{a}	4.08^{a}
	Transition	8.17^{b}	2.98^{b}	2.56^{b}	45.23^{c}	1.26^{bc}	1.92^{b}	3.48^{ba}	2.47^{a}	1.80^{a}	3.78^{a}	4.15^{a}
	In-Field	8.53^{a}	2.84^{b}	2.54^{b}	39.35^{d}	1.25^{c}	1.81^{c}	3.38^{b}	2.31^{a}	1.69^{b}	3.82^{a}	3.87^{a}
WW	Field Edge	9.31^{c}	3.36^{a}	2.92^{a}	45.92^{ba}	1.33^{a}	1.81^{a}	3.52^{a}	2.93^{a}	1.70^{ba}	3.57^{a}	4.23^{a}
	Turning	11.73^{b}	3.41^{a}	3.08^{a}	47.13^{a}	1.35^{a}	1.85^{a}	3.53^{a}	2.83^{a}	1.81^{ba}	3.50^{a}	4.08^{a}
	Transition	13.02^{a}	3.08^{ba}	2.59^{b}	42.15^{b}	1.32^{a}	1.80^{a}	3.47^{a}	2.79^{a}	1.88^{a}	3.36^{a}	3.74^{a}
	In-Field	13.35^{a}	2.88^{b}	2.43^{b}	36.18^{c}	1.27^{b}	1.73^{a}	3.37^{a}	3.05^{a}	1.66^{b}	3.33^{a}	3.72^{a}

This phenomenon of machinery used for cultivation and seedbed preparation in the upper layer negatively affecting soil structural condition in the lower layer, is also reported by Schafer-Landefeld (2004). With each machine pass, the risk of soil deformation and compaction at lower depths increases (Alakukku et al., 2003), highlighting the destructive impact of tillage operations on soil structure as found in other studies (Garbout et al., 2013; Askari et al., 2013). In the absence of any remedial soil structural work such as sub-soiling which may only alleviate problems to 450 mm (Batey, 2009), the effects of soil structural damage in this layer are long lasting (Alakukku et al., 2003), and the more pronounced the compacting effect, the greater the time required for soil structural regeneration to occur (Pagliai, 1998).

In the current study, visual soil evaluation methods (VESS and Double Spade) proved sensitive at detecting soil structural differences between zones, particularly at >250 mm soil depth (below plough depth). This was also noted in a smaller study by Emmet-Booth et al. (2019b) in the same temperate maritime climatic region. Progressive increases in *Sq* and *DS* were noted with increasing headland machine traffic. This indicated progressively poorer soil structural quality with zones of increasing traffic intensities. In the upper soil layer (0−250 mm) this was confirmed by shear resistance (SR) and to a lesser extent by bulk density. Considering the 250−400 mm soil depth, *DS* showed a significant zone effect suggesting structural changes caused by machine traffic differences. Similar to other studies (Berryman et al., 1982; Emmet-Booth et al., 2019b), this effect was not detected by many of the quantitative soil assessments. The ability of *Sq* and *DS* to assess the impact of traffic zones on aggregates, and other soil properties not assessed by quantitative measurements is beneficial, allowing early detection of structural damage. Also, visual techniques are less affected by soil moisture than soil strength measurements.

By analysing and presenting the data in terms of zones, the novel approach employed in this study considered each zone as a unique headland area and quantified the impact of specific machine traffic patterns on soil structure and crop performance. This contrasts with previous research and highlights the importance of why headlands cannot be considered as one homogeneous field area, nor can distance from the field edge be used in a simple response relationship to determine either soil structure or crop effects. This research clearly indicates that the factors contributing to yield loss on headlands differ between zones.

To reduce the risk of soil structural damage and subsequent yield impacts by the passage of machinery traffic, the use of low ground pressure tyres is recommended (Alakukku et al., 2003; Hanse et al., 2011; VDI, 2014). If machine choices are made based on the load bearing capacity of the soil, subsoil compaction can be avoided (VDI, 2014). Consideration also needs to be given to soil moisture conditions, under which operations occur (VDI, 2014), particularly in high clay content soils (Batey, 2009). Even marginal reductions in topsoil water content will reduce the compacting effect of a machine pass on the layers beneath (Gysi et al., 1999).

When considering crop performance, the recorded soil structural impact was accompanied by a yield effect on many of the sites, where reduced soil structural quality and yields were recorded at the turning zone when compared to the in-field area. The in-field zones of least machine traffic that indicated best soil structural quality also produced the highest grain yields for all crop types. Crop performance reduced on the field headlands following similar patterns as indicated by visual soil structural quality, but with the noteworthy exception of the field edge. The effects of soil compaction are generally negative for plant growth, leading to reduced yields (Arvidsson and Håkansson, 2014). This is also apparent from the influence of cone penetrometer in the multi-predictor grain yield models. Better correlations were documented with the inclusion of visual soil data for most crop types. This highlights their utility in assessing soil structural change that impacts growing conditions for each crop. Despite the negative impact of machinery traffic on soil structure, the analysis of headlands by zones enables us to see that soil

structure was not the only factor affecting crop yield. While the headland zones (field edge, turning & transition zones) had inferior soil structure and lower yields than the in-field area, the turning zone which had the greatest traffic intensity was not the lowest yielding zone. This result was recorded on most of the surveyed sites, highlighting the magnitude of the issue in the main cereal growing region of Ireland. Other factors such as variations in input application (Tsiouris and Marshall, 1998; Wilcox et al., 2000) or edge effects associated with crop boundaries are likely to contribute and warrant investigation.

This study hypothesised that the zone of poorest soil structure would have the lowest grain yields. While the turning zone of greatest traffic intensity returned the poorest soil scores, the zone of lowest crop yield was the field edge. Even though other studies report reduced headland yields (Cook and Ingle, 1997; Sparkes et al., 1998a; Wilcox et al., 2000), the methodology used in these studies did not allow the response in specific areas of the headland to be determined, and consequently the potential for different headland factors to contribute to a crop effect could not be identified. Other field edge headland factors such as shading and water competition from hedges or woods, weed ingress, damage by small grazing mammals (Speller et al., 1992) and, misplaced fertiliser (Tsiouris and Marshall, 1998) must also be considered.

The work reported in the current study suggests that even though the soil structural impact is not the primary cause of yield loss at the field edge, other field areas are affected. There is therefore potential to reduce the risk of soil structural degradation and spatial yield variability on headlands with amendments to machine management practices that observe soil limits for trafficking and cultivation events (Müller et al., 2011; VDI, 2014).

5. Conclusion

The current study addressed the extent and causes of headland effects on soil structure and crop performance, from a survey of tilled field headlands in a temperate maritime climate using a novel zone approach. This demonstrated the negative effect of increasing machinery traffic intensity on soil structure in some of the zones. Progressive changes for the majority of visual and quantitative soil assessments were observed with increasing levels of machinery traffic. The zone approach permitted areas of spatial difference to be assessed. It showed grain yields did not always follow zone trends in soil structure, where the field edge zone had the lowest crop yields despite having better soil structure quality than the turning zone. Consideration should be given to these field areas, where management practices other than machine traffic patterns necessitate review to determine the cause of crop loss at the field edge. Visual soil assessment methods present growers with a systematic methodology for determining the suitability of a soil for trafficking, increase their awareness of the impact of machine traffic on soil structure, and therefore highlight the impact of inappropriate field management.

From this work, it can be concluded that the use of zones, as designated by machinery operations enabled the variability in soil structural condition between different headland areas to be determined. While not all of the headland effects can be explained by soil structural impacts, future work should investigate the boundary features impacting headland traffic zone grain yields such as variability in fertiliser input applications. This is particularly important for the field edge zone, where machine traffic was shown to affect visually and quantitatively assessed soil structural conditions, and crop performance on tilled field headlands in a temperate maritime climate.

Declaration of Competing Interest

The authors report no declarations of interest.

Acknowledgements

This project was funded under a Teagasc Walsh Fellowship fund as part of the CTF-OPTIMOVE project funded by DAFM and Teagasc through the ICTAGRI Eranet. The authors wish to acknowledge the assistance of Brendan Burke, J.P. Emmet-Booth, Aline Mouthuy, Marine Pellentz and Pierre Retailleau.

References

Alakukku, L., Weisskopf, P., Chamen, W., Tijink, F., Van Der Linden, J., Pires, S., Sommer, C., Spoor, G., 2003. Prevention strategies for field traffic-induced subsoil compaction: a review: part 1. Machine/soil interactions. Soil Tillage Res. 73, 145–160.
Allmaras, R., Kraft, J., Miller, D., 1988. Effects of soil compaction and incorporated crop residue on root health. Annu. Rev. Phytopathol. 26, 219–243.
Anken, T., Holpp, M., Weisskopf, P., 2016. Controlled Traffic Farming Improves Soil Physical Parameters. CIGR-EurAgEng, Aarhus, Denmark.
Ansorge, D., Godwin, R., 2007. The effect of tyres and a rubber track at high axle loads on soil compaction, Part 1: single axle-studies. Biosyst. Eng. 98, 115–126.
Arvidsson, J., Håkansson, I., 2014. Response of different crops to soil compaction—short-term effects in Swedish field experiments. Soil Tillage Res. 138, 56–63.
Arvidsson, J., Keller, T., 2007. Soil stress as affected by wheel load and tyre inflation pressure. Soil Tillage Res. 96, 284–291.
Askari, M.S., Cui, J., Holden, N.M., 2013. The visual evaluation of soil structure under arable management. Soil Tillage Res. 134, 1–10.
Bachmann, J., Hartge, K.H., 2006. Estimating soil stress distribution by using depth-dependent soil bulk-density data. J. Plant Nutr. Soil Sci. 169, 233–238.
Ball, B., Batey, T., Munkholm, L.J., 2007. Field assessment of soil structural quality–a development of the Peerlkamp test. Soil Use Manag. 23, 329–337.
Ball, B., Batey, T., Munkholm, L.J., Guimarães, R., Boizard, H., Mckenzie, D., Peigné, J., Tormena, C., Hargreaves, P., 2015. The numeric visual evaluation of subsoil structure (SubVESS) under agricultural production. Soil Tillage Res. 148, 85–96.
Bartholomew, P., Williams, R., 2010. Effects of soil bulk density and strength on seedling growth of annual ryegrass and tall fescue in controlled environment. Grass Forage Sci. 65, 348–357.
Batey, T., 2009. Soil compaction and soil management–a review. Soil Use Manage. 25, 335–345.
Bell, L.W., Kirkegaard, J.A., Swan, A., Hunt, J.R., Huth, N.I., Fettell, N.A., 2011. Impacts of soil damage by grazing livestock on crop productivity. Soil Tillage Res. 113, 19–29.
Berryman, C., Davies, D., Evans, C., Harrod, M., Hughes, A., Skinner, R., Swain, R., Soane, D., 1982. Techniques for measuring soil physical properties. Techniques for Measuring Soil Physical Properties, p. 18.
Boatman, N., 1992. Effects of herbicide use, fungicide use and position in the field on the yield and yield components of spring barley. J. Agric. Sci. 118, 17–28.
Boatman, N., Sotherton, N., 1988. The agronomic consequences and costs of managing field margins for game and wildlife conservation. Asp. Appl. Biol.
Bochtis, D., Vougioukas, S., 2008. Minimising the non-working distance travelled by machines operating in a headland field pattern. Biosyst. Eng. 101, 1–12.
Botta, G., Jorajuria, D., Balbuena, R., Rosatto, H., 2004. Mechanical and cropping behavior of direct drilled soil under different traffic intensities: effect on soybean (Glycine max L.) yields. Soil Tillage Res. 78, 53–58.
Botta, G., Becerra, A.T., Tourn, F.B., 2009. Effect of the number of tractor passes on soil rut depth and compaction in two tillage regimes. Soil Tillage Res. 103, 381–386.
Botta, G., Tolón-Becerra, A., Lastra-Bravo, X., Tourn, M., Balbuena, R., Rivero, D., 2013. Continuous application of direct sowing: traffic effect on subsoil compaction and maize (Zea mays L.) yields in Argentinean Pampas. Soil Tillage Res. 134, 111–120.
Brady, N.C., Weil, R.R., Weil, R.R., 2008. The Nature and Properties of Soils. Prentice Hall, Upper Saddle River, NJ.
Burke, B., Mcdonnell, K., Forristal, D., 2018. A Study of Machine Dynamics on Headlands in Irish Tillage Farms and Its Impact on Efficiency and Traffic Patterns. Master of Science (Agriculture), University College Dublin.
Chamen, T., Cottage, C.C., Maulden, B., 2006. Controlled traffic" farming: literature review and appraisal of potential use in the UK. HGCA Res. Rev. 59.
Cook, S., Ingle, S., 1997. The effect of boundary features at the field margins on yields of winter wheat. Asp. Appl. Biol.
Cook, A., Marriott, C., Seel, W., Mullins, C., 1996. Effects of soil mechanical impedance on root and shoot growth of Lolium perenne L., Agrostis capillaris and Trifolium repens L. J. Exp. Bot. 47, 1075–1084.
Ehlers, W., Goss, M., 2016. Water Dynamics in Plant Production. CABI Publishing, Oxon, UK.
Emmet-Booth, J., Forristal, P., Fenton, O., Holden, N., 2016. The visual evaluation of soil structure At varying soil moisture contents At lyons estate. Biosyst. Food Eng. Res. Rev. 21, 174.
Emmet-Booth, J., Forristal, P., Fenton, O., Bondi, G., Holden, N., 2019a. Visual soil evaluation–spade vs. profile methods and the information conveyed for soil management. Soil Tillage Res. 187, 135–143.

Emmet-Booth, J., Holden, N., Fenton, O., Bondi, G., Forristal, P., 2019b. Exploring the sensitivity of visual soil evaluation to traffic-induced soil compaction. Geoderma Reg. e00243.
Emmet-Booth, J., Forristal, P., Fenton, O., Ball, B., Holden, N., 2016. A review of visual soil evaluation techniques for soil structure. Soil Use Manage. 32, 623–634.
Emmet-Booth, J., Bondi, G., Fenton, O., Forristal, P., Jeuken, E., Creamer, R., Holden, N., 2018. Grass VESS: a modification of the visual evaluation of soil structure method for grasslands. Soil Use Manage. 34, 37–47.
Garbout, A., Munkholm, L.J., Hansen, S.B., 2013. Tillage effects on topsoil structural quality assessed using X-ray CT, soil cores and visual soil evaluation. Soil Tillage Res. 128, 104–109.
Grossman, R., Reinsch, T., 2002. Bulk density and linear extensibility. Methods of Soil Analysis: Part 4 Physical Methods, pp. 201–228.
Guimarães, R., Ball, B., Tormena, C., 2011. Improvements in the visual evaluation of soil structure. Soil Use Manage. 27, 395–403.
Gysi, M., Ott, A., Flühler, H., 1999. Influence of single passes with high wheel load on a structured, unploughed sandy loam soil. Soil Tillage Res. 52, 141–151.
Håkansson, I., 2005. Machinery-induced Compaction of Arable Soils Incidence, Consequences and Counter-measures. Swedish University of Agricultural Sciences, Department of Soil Sciences. Uppsala, Sweden. Report no. 109, 153 pp.
Håkansson, I., Medvedev, V., 1995. Protection of soils from mechanical overloading by establishing limits for stresses caused by heavy vehicles. Soil Tillage Res. 35, 85–97.
Hanse, B., Vermeulen, G., Tijink, F., Koch, H.-J., Märländer, B., 2011. Analysis of soil characteristics, soil management and sugar yield on top and averagely managed farms growing sugar beet (Beta vulgaris L.) in the Netherlands. Soil Tillage Res. 117, 61–68.
Ishaq, M., Hassan, A., Saeed, M., Ibrahim, M., Lal, R., 2001a. Subsoil compaction effects on crops in Punjab, Pakistan: I. Soil physical properties and crop yield. Soil Tillage Res. 59, 57–65.
Ishaq, M., Ibrahim, M., Hassan, A., Saeed, M., Lal, R., 2001b. Subsoil compaction effects on crops in Punjab, Pakistan: II. Root growth and nutrient uptake of wheat and sorghum. Soil Tillage Res. 60, 153–161.
Kennedy, S., 2015. Identifying Constraints to Increasing Yield Potential of Spring Barley. Doctor of Philosophy. The University of Edinburgh.
Kuemmel, B., 2003. Theoretical investigation of the effects of field margin and hedges on crop yields. Agric. Ecosyst. Environ. 95, 387–392.
Kumhála, F., Gutu, D., Hůla, J., Chyba, J., Kovaříček, P., Kroulík, M., Kvíz, Z., Mašek, J., Vláśková, M., 2013. Technology of controlled traffic farming on fields. Certificated Methodology.
Logsdon, S., Cambardella, C., 2000. Temporal changes in small depth-incremental soil bulk density. Soil Sci. Soc. Am. J. 64, 710–714.
Mchugh, A., Tullberg, J., Freebairn, D., 2009. Controlled traffic farming restores soil structure. Soil Tillage Res. 104, 164–172.
Muckel, G.B., Mausbach, M.J., 1996. Soil quality information sheets. Methods for Assessing Soil Quality, pp. 393–400.
Mueller, L., Kay, B.D., Hu, C., Li, Y., Schindler, U., Behrendt, A., Shepherd, T.G., Ball, B. C., 2009. Visual assessment of soil structure: evaluation of methodologies on sites in Canada, China and Germany: part I: comparing visual methods and linking them with soil physical data and grain yield of cereals. Soil Tillage Res. 103, 178–187.
Mueller, L., Shepherd, G., Schindler, U., Ball, B.C., Munkholm, L.J., Hennings, V., Smolentseva, E., Rukhovic, O., Lukin, S., Hu, C., 2013. Evaluation of soil structure in the framework of an overall soil quality rating. Soil Tillage Res. 127, 74–84.
Müller, L., Lipiec, J., Kornecki, T.S., Gebhardt, S., 2011. Trafficability and workability of soils. Encyclopedia of Agrophysics. Springer.
Murphy, B.W., Crawford, M.H., Duncan, D.A., Mckenzie, D.C., Koen, T.B., 2013. The use of visual soil assessment schemes to evaluate surface structure in a soil monitoring program. Soil Tillage Res. 127, 3–12.
Newell-Price, J., Whittingham, M., Chambers, B., Peel, S., 2013. Visual soil evaluation in relation to measured soil physical properties in a survey of grassland soil compaction in England and Wales. Soil Tillage Res. 127, 65–73.
O'flynn, M.G., Finnan, J.M., Curley, E.M., Mcdonnell, K.P., 2014. Reducing crop damage and yield loss in late harvests of Miscanthus× giganteus. Soil Tillage Res. 140, 8–19.
Pagliai, M., 1998. Changes of Pore System Following Soil Compaction. Experiences With the Impact and Prevention of Subsoil Compaction in the European Community.
Schäfer-Landefeld, L., Brandhuber, R., Fenner, S., Koch, H.-J., Stockfisch, N., 2004. Effects of agricultural machinery with high axle load on soil properties of normally managed fields. Soil Tillage Res. 75, 75–86.
Scholefield, D., Hall, D., 1985. A method to measure the susceptibility of pasture soils to poaching by cattle. Soil Use Manage. 1, 134–138.
Sparkes, D., Jaggard, K., Ramsden, S., Scott, R., 1998a. The effect of field margins on the yield of sugar beet and cereal crops. Ann. Appl. Biol. 132, 129–142.
Sparkes, D., Ramsden, S., Jaggard, K., Scott, R., 1998b. The case for headland set-aside: consideration of whole-farm gross margins and grain production on two farms with contrasting rotations. Ann. Appl. Biol. 133, 245–256.
Speller, C., Cleal, R., Runham, S., 1992. A comparison of winter wheat yields from headlands with other positions in five fen peat fields. Monogr.-Br. Crop Prot. Council 47.
Teagasc, 2018. Teagasc - About [Online]. Available: https://www.teagasc.ie/ [Accessed 20 11 2018].
Tebrügge, F., Düring, R.-A., 1999. Reducing tillage intensity—a review of results from a long-term study in Germany. Soil Tillage Res. 53, 15–28.
To, J., Kay, B., 2005. Variation in penetrometer resistance with soil properties: the contribution of effective stress and implications for pedotransfer functions. Geoderma 126, 261–276.
Tsiouris, S., Marshall, E., 1998. Observations on patterns of granular fertiliser deposition beside hedges and its likely effects on the botanical composition of field margins. Ann. Appl. Biol. 132, 115–127.
Usda, 2018. Soil Texture Calculator [Online]. Available: https://www.nrcs.usda.gov/wps/portal/nrcs/detail/soils/research/guide/?cid=nrcs142p2_054167 [Accessed 12 07 2018].
Van Den Akker, J., Schjønning, P., 2004. Subsoil compaction and ways to prevent it. Managing Soil Quality: Challenges in Modern Agriculture, pp. 163–184.
Vdi, 2014. Machine Operation With Regard to the Trafficability of Soils Used for Agriculture. Verein Deutscher Ingenieure, Düsseldorf. July 2014.
Vieweger, A., 2016. CP 107b - Growing Resilient Efficient and Thriving Soils (GREAT) Soils [Online]. Available: https://horticulture.ahdb.org.uk/project/growing-resilient-efficient-and-thriving-soils-great-soils [Accessed 17 04 2019].
Ward, M., Forristal, P., Mc Donnell, K., 2020. The impact of field headlands on wheat and barley performance in a cool Atlantic climate as assessed in 40 Irish tillage fields (IN PRESS). Irish J. Agric. Food Res.
Welch, R.Y., Behnke, G.D., Davis, A.S., Masiunas, J., Villamil, M.B., 2016. Using cover crops in headlands of organic grain farms: effects on soil properties, weeds and crop yields. Agric. Ecosyst. Environ. 216, 322–332.
Wilcox, A., Perry, N., Boatman, N., Chaney, K., 2000. Factors affecting the yield of winter cereals in crop margins. J. Agric. Sci. 135, 335–346.